Triply differential cross section for ionization in ion-atom collisions

G. Gasaneo, W. Cravero,* M. D. Sánchez,† and C. R. Garibotti
CONICET and Centro Atómico Bariloche, 8400 Bariloche, Argentina
(Received 8 May 1995; revised manuscript received 29 September 1995)

First Born approximation (FBA) and continuum-distorted-wave–eikonal-initial-state (CDW-EIS) approximation are used to calculate the cross section that is triply differential (TDCS) in the energy and angle of the emitted electron and scattered projectile for proton impact ionization of atomic hydrogen. The TDCS shows different prominent features, whose origin is examined on the basis of the results given by FBA calculations and reported for different physical effects. We discuss how these features are related to those present in the doubly differential cross section (DDCS). [S1050-2947(96)04106-6]

PACS number(s): 34.50.−s

I. INTRODUCTION

The FBA was first applied for the ionization of atoms by ion impact by Bates and Griffing (1953) [1]. Their results for the total cross section for ionization of atomic hydrogen by protons agree fairly well with the experiments.

The first experimental measurements of the doubly differential cross section in the electron energy and angle (DDCS) were obtained while the discussion on the total cross-section behavior was still open, regarding its dependence on the relevant parameters [2]. Nowadays, fairly detailed DDCSs, both theoretical and experimental, for ion-impact and electron-impact ionization are already available for a large number of targets [3,4].

The FBA has been applied to the evaluation of the DDCS for high-energy and low charge projectiles [2,5,9]. The electron spectra are described qualitatively well, particularly, in the soft electron and binary encounter regions. The description fails when the Born factor Z_P/v increases, and does not reproduce the electron capture to the continuum (ECC) structure because the FBA does not take into account the projectile-electron interaction in the exit channel [6–8]. For these reasons, many authors contrast the result of this theory with other more sophisticated ones, like the continuum-distorted-wave–eikonal-initial-state approximation (CDW-EIS) [10–12].

The most detailed information possible on an ionizing collision is provided by the triply differential cross section (TDCS), defined as $d^3\sigma/dE_k d\Omega_k d\Omega_K$, where $dE_k = k dk$ and $d\Omega_k$ give, respectively, the energy and the solid angle element of the outgoing electron, and $d\Omega_K$ specifies the solid angle element of the scattered projectile. The TDCS for electron-impact ionization has been measured [13] and evaluated, but no attention has been paid to the ion-atom case. The purpose of this work is to begin with the analysis of the TDCS for proton-impact ionization, although experimental data are not available for this process yet.

The paper is organized as follows: The transition matrix element in the FBA and CDW-EIS approximation are presented and compared in Sec. II. In Sec. III a detailed analysis of the different structures that come from the TDCS in the FBA is presented. Finally, Sec. IV summarizes our conclusions.

II. TRIPLY DIFFERENTIAL CROSS SECTION

We consider the ionization of a neutral hydrogen atom by a fast charged particle P^{Z+}, namely

$$P^{Z+} + \mathrm{H}(1s) \rightarrow P^{Z+} + \mathrm{H}^+ + e. \tag{1}$$

The triply differential cross section in energy and ejection angle of the electron, and direction of the outgoing proton for this process are given by

$$\frac{d^3\sigma}{dE_k d\Omega_k d\Omega_K} = (2\pi)^4 \frac{\nu k}{|\mathbf{K}_i|} |T_{if}|^2 \delta(E_f - E_i), \tag{2}$$

where ν is the reduced mass of the proton-atom system, $\mathbf{K}_i$ the momentum of the incident particle, T_{if} the transition amplitude, and $\delta(E_f - E_i)$ expresses the energy conservation of the system.

In the FBA, the transition amplitude in Eq. (2), is [14]

$$T^{\mathrm{FBA}} = \langle \varphi_{\mathbf{K}_f} \psi_{\mathbf{k}}^- | V_P | \varphi_{\mathbf{K}_i} \phi_i \rangle, \tag{3}$$

where V_P is the electron-projectile Coulomb potential, $\psi_{\mathbf{k}}^-$ is a hydrogenic continuum wave function centered in the target, $\varphi_{\mathbf{K}_{i,f}}$ are plane waves describing the free relative internuclear motion, and ϕ_i is the initial bound state of the atom.

On the other hand, the transition amplitude in the CDW-EIS approximation reads [15]

$$T^{\mathrm{CDW\text{-}EIS}} = \langle \varphi_{\mathbf{K}_f} \psi_{\mathbf{k}}^- \chi_f^{\mathrm{CDW}} | -\nabla_{\mathbf{r}_T} \cdot \nabla_{\mathbf{r}_p} | \varphi_{\mathbf{K}_i} \phi_i \chi_i^{\mathrm{EIS}} \rangle, \tag{4}$$

where $(-\nabla_{\mathbf{r}_T} \cdot \nabla_{\mathbf{r}_P})$ is the CDW perturbation, i.e., the non-orthogonal kinetic energy that connects the electron with the target nucleus T and with the projectile P [15]. The final state includes the projectile distortion through the function χ_f^{CDW}. The initial state obeys the correct asymptotic condition, including the eikonal phase χ_i^{EIS}, which describes the asymptotic interaction between the incoming projectile and the initial bound electron.

*Also at Universidad Nacional del Comahue, Quintral 1250, 8400 Bariloche, Argentina.

†Also at Universidad Nacional del Sur, Av. Pellegrini 250, 8000 Bahía Blanca, Argentina.

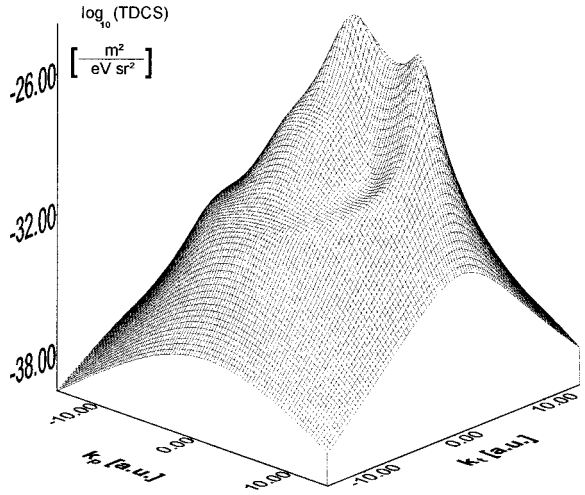

FIG. 1. Decimal logarithm of the triply differential cross section (TDCS), in the first Born approximation, as a function of the momentum $\mathbf{k}$ of the electron. The axes $\mathbf{k}_p$ and $\mathbf{k}_t$ are the momenta parallel and transversal to the initial direction of the projectile. The energy of the projectile is 500 keV/amu. The final direction of the projectile momentum is fixed at 4×10^{-4} deg.

From Eqs. (3) and (4) we have calculated the TDCS as a function of the electron angle and energy of emission and for each fixed deflection angle of the projectile for the proton-hydrogen collision. The general shape of the TDCS in the electron momentum space, as given by the FBA, is shown in Fig. 1, for $E_i=500$ keV/amu and when the proton deflected at a 4×10^{-4} angle. We observe four prominent features in the electron spectra, i.e., two peaks and two rings. The positions and physical origin of these features will be discussed in the next section.

Comparison of the FBA and CDW-EIS approaches is performed in Figs. 2(a), 2(b), and 2(c), for the proton-hydrogen collision at 500 keV/amu and undeflected projectile. We observe that both approximations agree quite well, except for the known electron capture to the continuum (ECC) peak given by CDW-EIS. Similar results are obtained for other impact energies and other final projectile angles. Consequently, based on the similar results given by both theories, we will carry on the analysis of the TDCS structures employing the FBA, because its mathematical simplicity allows us to perform most calculations analytically. However, we should note that increasing differences between both approximations could be expected when the projectile charge is increased. In this case, the electron-ion interaction is very strong, and a first-order perturbative description becomes incorrect. This is also the case for low projectile impact energies [6].

III. ANALYSIS OF THE TDCS STRUCTURES

The transition matrix element in Eq. (3) can be expressed as

$$|T_{fi}|^2=8\pi[\widetilde{V}_P(q)]^2|N(\xi)|^2\exp\left\{-2\xi\tan^{-1}\left[\frac{2\mu Z_i k}{q^2+Z_i^2-k^2}\right]\right\}\times F(\mathbf{k},\mathbf{q})G(k,q)|\widetilde{\phi}_i(\mathbf{q}-\mathbf{k})|^2, \quad (5)$$

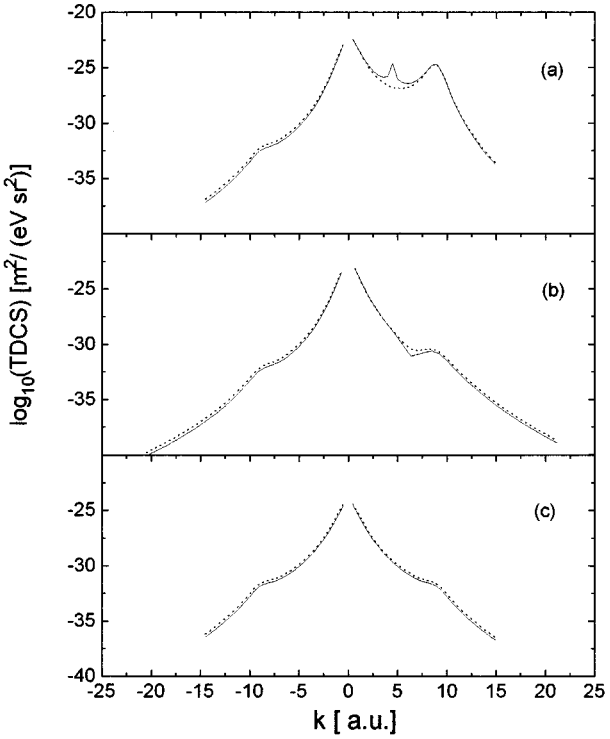

FIG. 2. Decimal logarithm of the triply differential cross section (TDCS) in first Born approximation, dotted line, and continuum-distorted-wave-eikonal-initial state, solid line, as a function of the momentum $\mathbf{k}$ of the electron. The deflection angle and energy of the projectile are 0° and 500 keV/amu, respectively. The emission angle of the electron is (a) 0°, (b) 45°, and (c) 90°.

where

$$F(\mathbf{k},\mathbf{q})=[q^2(Z_i+Z_1)-(k^2-(\mu Z_i)^2)(Z_i-Z_1)-2Z_1\mathbf{q}\cdot\mathbf{k}]^2+\left(\frac{2Z_iZ_1\mu}{k}\right)^2\left[k^2\left(\frac{Z_i}{Z_1}-1\right)-\mathbf{q}\cdot\mathbf{k}\right]^2, \quad (6)$$

$$G(k,q)=\frac{1}{[(\mu Z_i)^2+(q+k)^2][(\mu Z_i)^2+(q-k)^2]}, \quad (7)$$

$$\widetilde{\phi}_i(\mathbf{q}-\mathbf{k})=\frac{2\sqrt{2}\pi(\mu Z_i)^{5/2}}{[(\mu Z_i)^2+(\mathbf{q}-\mathbf{k})^2]^2}, \quad (8)$$

$$\widetilde{V}_P(q)=\frac{4\pi Z_P}{q^2}, \quad (9)$$

where $\mathbf{q}=\mathbf{K}_i-\mathbf{K}_f$, and Z_i and Z_1 are the target core charges assumed for the initial bound $1s$, and final continuum hydrogenic states, respectively. They are equal for the H target, but Z_1 can be replaced by an effective charge to model passive electron screening in multielectronic targets by hydrogenic wave functions. This is a usual assumption in ion-atom ionization calculation, and allows us to extend easily our analysis to other targets.

Equation (5) was first used in 1930 by Bethe for the evaluation of cross sections for electron-impact ionization of atomic hydrogen [16]. Due to the lack of measurements of the TDCS Eq. (5) is integrated over the momentum transfer

q to obtain the DDCS, which is the usually studied quantity. That integration smoothed many of the features of the TDCS. Here we will analyze Eq. (5) to get conclusions about the electron spectra that we can expect from future coincidence experiments.

The factors in Eq. (5) can be associated with different structures in the transition matrix $N(\xi)$, where $\xi=Z_1/k$ is the Coulomb factor, which arises from the normalization of the scattering wave function, and $|\widetilde{V}_P(q)|^2$ is the Fourier transform of the projectile potential and is essentially the Coulomb differential cross section for the scattering of the projectile off the target. The divergence of $N(\xi)$ for $k\rightarrow 0$, gives the soft electron peak in the cross section $d^3\sigma/d\mathbf{k}\,d\Omega_K$, but it is hidden by the factor k in Eq. (2). The factors $G(k,q)$ and $|\widetilde{\phi}_i(\mathbf{q}-\mathbf{k})|^2$ show maximum values when determinated kinematic relations among $\mathbf{K}_i$, $\mathbf{K}_f$, and $\mathbf{k}$ are given. Instead, the factor $F(\mathbf{k},\mathbf{q})$ is proportional to the bound-continuum oscillator strength related to dynamical properties of the colliding system.

The factor $G(k,q)$ attains its maximum value when $q=k$, which requires that

$$k^2=\frac{2}{\left(1-\frac{\nu}{\mu}\right)^2}\left(\left(1+\frac{\nu}{\mu}\sin^2\Gamma\right)K_i^2+\left(1+\frac{\nu}{\mu}\right)\nu\epsilon \pm K_i\cos\Gamma\left\{K_i^2\left[1-\left(\frac{\nu}{\mu}\right)\sin\Gamma\right]^2+2\nu\epsilon\left(1+\frac{\nu}{\mu}\right)\right\}^{1/2}\right), \tag{10}$$

where ν and μ are the reduced masses of the projectile and electron-nucleus target system, respectively, Γ is the projectile outgoing angle on the same system, and ϵ is the binding energy in the initial state. For an hydrogenic $1s$-state. $\epsilon=(\mu Z_i)^2$. Therefore, we have two values of k where $G(k,q)$ has a maximum, corresponding to two concentric circles in k space centered in $k=0$.

The factor $|\widetilde{\phi}_i(\mathbf{q}-\mathbf{k})|^2$ attains its maximum when $\mathbf{q}=\mathbf{k}$. This condition is equivalent to momentum conservation in a projectile-electron binary collision, which results from assuming an infinite mass for the target core. The condition requires that

$$k^{\pm}=\frac{1}{1+\frac{\nu}{\mu}}\left\{K_i\cos\theta\pm\left[K_i^2\cos^2\theta+2\nu\epsilon\left(1+\frac{\nu}{\mu}\right)\right]^{1/2}\right\}, \tag{11}$$

which represents a circle in the momentum plane, centered in the velocity of the projectile with radius smaller than this velocity. Therefore, this circle does not touch the point $k=0$. Here θ is the emission angle of the electron relative to the incidence direction. For a given value of Γ, the condition $\mathbf{q}=\mathbf{k}$ is satisfied in two points located on the circle. These points are situated in the crossing of the circles given by Eqs. (10) and (11). We sketch these features in Fig. 3. The integration over all momentum-transfer directions, as required for the evaluation of the DDCS, adds the contributions of these binary peaks and gives the origin to the known binary circle, which in the limit $\epsilon\rightarrow 0$ has the radius

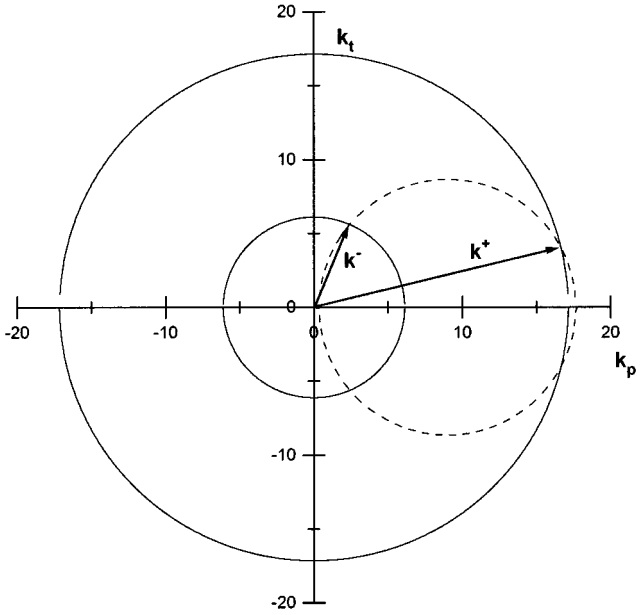

FIG. 3. Location of the maxima of the TDCS in the electron momentum plane for a fixed projectile outgoing angle. The vectors $\mathbf{k}^+$ and $\mathbf{k}^-$ are the directions of the electron resulting from the binary collision with the projectile, as given by Eq. (11). The tips of these vectors move along the dashed circle as the projectile outgoing angle changes. These binary electrons are sent with the momenta located in the continuous circles after a second collision with the target, as given by Eq. (10).

$$k=2\frac{K_i}{\nu}\cos\theta. \tag{12}$$

The Coulomb wave function introduced for the description of the electron-target nucleus final continuum state contains infinite perturbative orders in the electron-target interaction. In a naive sense, it can be expanded from

$$|\psi_{\mathbf{k}}^-\rangle=|\varphi_{\mathbf{k}}\rangle+G_0V_T|\psi_{\mathbf{k}}^-\rangle,$$

where V_T is the electron-target potential, which in Eq. (3) gives

$$T^{\mathrm{FBA}}=\langle\varphi_{\mathbf{K}_f}\varphi_{\mathbf{k}}|(1+V_T+V_TG_0V_TG_0+\cdots)V_P|\varphi_{\mathbf{K}_i}\phi_i\rangle. \tag{13}$$

The first term in this expansion gives the plane wave approximation:

$$|T^{\mathrm{PW}}|^2\approx|\widetilde{V}_P(q)|^2|\widetilde{\phi}_i(\mathbf{q}-\mathbf{k})|^2.$$

The remaining term shows that after being hit by the projectile, the electron suffers successive collisions with the target, which are not present in the plane-wave approximation [17]. The function $G(k,q)$ accounts for these terms and therefore, the maxima placed in the circles given by Eq. (10) can be interpreted as resulting from a further collision of the binary electrons with the target ion, in this case a proton. In a first collision with the projectile, the electron is sent in the

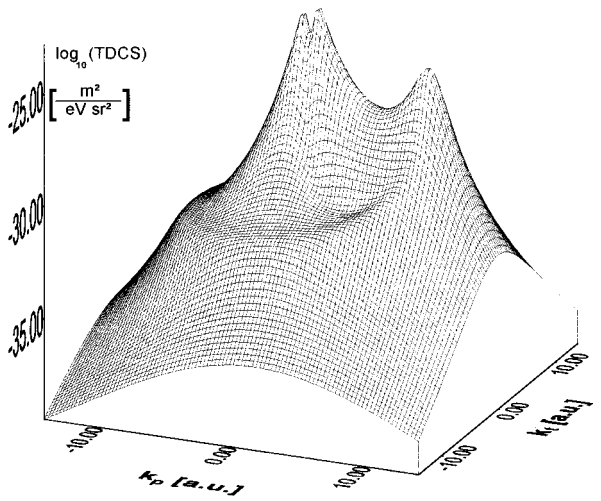

FIG. 4. Decimal logarithm of base 10 of the triply differential cross section (TDCS), in the first Born approximation as a function of the momentum **k** of the electron, for a collision energy of 500 keV/amu and the projectile continuing in the forward direction after the collision ($\mathbf{K}_i/\mathbf{K}_f$).

direction θ with momentum given by Eq. (11), then it collides with the target and is dispersed in the circles given by Eq. (10).

We should note that the expansion Eq. (13), is mathematically incorrect because the nonhomogeneous term of the Lippman-Schwinger equation (LSE) for the Coulomb wave is an asymptotically distorted wave, as has been shown by different authors [18]. However, this asymptotic behavior will not modify the physical interpretation given to the maxima.

Now let us consider the factor $F(\mathbf{k},\mathbf{q})$, which presents a sharp minimum. Calling α the angle between **q** and **k**, the position of that minimum is given by

$$\cos\alpha = \frac{(Z_i+Z_1)kq}{2Z_1(k^2+Z_i^2\mu^2)} - \frac{(Z_i-Z_1)k}{2Z_1 q}, \tag{14}$$

when $\mathbf{K}_f$ and **k** are in the same plane the location of the minimum is along a curve in the electron momentum plane given by

$$\sin\theta = \pm\frac{(K_f\sin(\alpha\pm\Gamma)-K_i\sin\alpha}{q}. \tag{15}$$

For given K_i and fixed Γ, this equation and energy conservation give a relation $k=k(\theta)$.

The + and − sign in Eq. (15) correspond to the tracks of the curve located in the upper and lower half of the electron momentum plane. When the projectile is scattered in the forward direction ($\Gamma=0$), and we assume $Z_1=Z_i$, the minimum extends along a circular slot, as we can observe in Fig. 4. We note that the shape of this curve depends on the charge assumed in the final Coulomb continuum state. For $k\to 0$ the factor $F(\mathbf{k},\mathbf{q})$ appears as

$$A + B\cos^2\alpha, \tag{16}$$

which by integration over all momentum transfer directions, gives

$$A + BP_2(\cos\theta), \tag{17}$$

i.e., the characteristic shape of the soft electron peak in the Born approximation for the DDCS [19]. This splits the soft electron peak in the so-called direct and recoil peaks. However, we should note that the mechanisms contributing to each of these peaks are different. This can be shown from the former discussion. Let us consider a simple case where $\hat{\mathbf{K}}_f=\hat{\mathbf{K}}_i$, such that Eq. (10) reduces to

$$k = \frac{1}{\left(1+\frac{\nu}{\mu}\right)^2}\left\{K_i^2 \pm \left[K_i^2 + 2\nu\epsilon\left(1+\frac{\nu}{\mu}\right)\right]^{1/2}\right\}, \tag{18}$$

giving two circles tangent to the binary one; they are shown by a solid line in Fig. 3. The inner circle has a radius given by the minus sign in Eq. (18). Meanwhile, the condition $\mathbf{q}=\mathbf{k}$ yields a peak over the circle in the forward direction. Both features are modulated by Eq. (16) and overlap to the $1/k$ divergence due to the Coulomb factor. Therefore, the direct and recoil peak have contributions from the binary process and from high perturbative orders, respectively.

In Eq. (6) the initial charge and final charge of the target were split. We have an important reason to do this. The final charge of the target appears only in $F(\mathbf{k},\mathbf{q})$ and in the Coulomb factor $N(\xi)$. We must note, therefore, that the modulator effect of factor F depends of the final charge of the target, and furthermore, changes in this residual charge do not produce changes in the general features of the TDCS. The importance of this observation is not evident in the proton-hydrogen collision process, in which the initial charge and final charge of the target are equal, but is relevant in a process where effective charges like the proton-helium collision, are usually different in the initial and final target wave functions.

IV. CONCLUSIONS

We studied the TDCS within the first Born approximation giving a description of the collision process for all **k** and **q**. We assume that the active electron is described by Coulomb states with different charges before and after emission. This is the usual assumption in ion-atom ionization calculations, when the passive electrons are assumed to produce a screening of the nuclear charge, which is partial in the initial bound state and complete in the final state of the active electron. This TDCS is composed of different factors that can be associated with particular physical processes. The Coulomb factor, due to the zero-energy resonance of the electron-target core potential, gives the soft electron peak; the Fourier transform of the initial state describes the binary ion-electron collision and produces two peaks in the electron velocity space, with location depending on the momentum transfer. The factor $G(k,q)$ is related to the process of double collision: first the bound electron hit by the incident ion is sent to the binary peak; and next these binary electrons hit on the target, giving rise to maxima along two rings in the velocity space. The radii of these rings depend on the angular deviation of the projectile. Integration over the momentum transfer in the evaluation of the DDCS adds these rings and leads to a hill for $k\approx 2K_i/\nu$. Recently, indirect experimental evi-

dence of this double collision mechanism has been presented [20]. The form factor $F(\mathbf{k},\mathbf{q})$ produces a slot in the distribution that surrounds the binary peaks on the TDCS. Its shape depends on the momentum transfer and the effective charges of the target core assumed to act on the electron in the initial and final states. This gives the characteristic dipolar shape of the DDCS in the soft electron peak [18].

The first Born approximation does not account properly for the electron-projectile interaction. In fact, it does not include the ECC cusp, soft electron asymmetry, and two-center effects. However, it allows for analytic discussion as presented here, which reveals a set of features in the TDCS, not observable when the DDCS is considered. The TDCS evidences the structure richness of the three-particle dynamics.

ACKNOWLEDGMENTS

This work has been partially supported by the CONICET, Argentina. We thank Dr. R. Barrachina and S. Suárez for useful discussions.

[1] D. R. Bates and G. Griffing, Proc. Phys. Soc. London Sect. A **66**, 961 (1953).
[2] M. Rudd and T. Jorgensen, Phys. Rev. **131**, 666 (1963).
[3] M. Rudd, Y. K. Kim, D. H. Madison, and T. J. Gay, Rev. Mod. Phys. **64**, 441 (1992).
[4] E. W. Mc Daniel, *Atomic Collision—Electron and Photon Projectiles* (Wiley, New York, 1989), Chap. 6.
[5] M. E. Rudd, C. A. Sautter, and C. L. Bailey, Phys. Rev. **20**, 151 (1966).
[6] S. T. Manson, L. H. Toburen, D. H. Madison, and N. Stolterforht, Phys. Rev. A **12**, 151 (1975).
[7] A. Salin, J. Phys. B **2**, 631 (1969).
[8] K. Dettmann, K. G. Harrison, and M. W. Lucas, J. Phys. B **37**, 269 (1974).
[9] M. Rudd, L. Toburen, and N. Stolterforht, At. Data Nucl. Data Tables **18**, 413 (1976); **23**, 405 (1979).
[10] P. Fainstein, V. Ponce, and R. Rivarola, J. Phys. B **21**, 287 (1988).
[11] D. S. F. Crothers and J. F. McCann, J. Phys B **16**, 3229 (1983).
[12] P. Fainstein, G. Bernardi, C. R. Garibotti, and S. Suárez, Europhys. Lett. (1988).
[13] H. Ehrhardt, G. Knoth, P. Schemmer, and K. Jung, Phys. Lett. **110A**, 92 (1985).
[14] M. R. C. McDowell and J. P. Coleman, *Introduction to the Theory of Ion-Atom Collision* (North-Holland, Amsterdam, 1970).
[15] D. S. F. Crothers and L. J. Dubé, Adv. At. Mol. Opt. Phys. **30**, 287 (1993).
[16] H. Bethe, Ann. Physics **5**, 325 (1930).
[17] J. S. Briggs, Comments At. Mol. Phys. **23**, 155 (1989).
[18] H. van Haeringen, J. Math. Phys. **17**, 995 (1976).
[19] J. S. Briggs and M. H. Day, J. Phys. B **13**, 4797 (1980).
[20] S. Suárez, W. R. Cravero R. Barrachina, C. R. Garibotti, W. Meckbach, R. Maier, M. Tobisch, and K. O. Groneveld (unpublished).